Intramolecular ^{13}C pattern in hexoses from autotrophic and heterotrophic C_3 plant tissues

Alexis Gilbert[a,b,1,2], Richard J. Robins[a], Gérald S. Remaud[a], and Guillaume G. B. Tcherkez[b,c]

[a]Interdisciplinary Chemistry: Synthesis, Analysis, Modeling, L'Université Nantes Angers Le Mans, Centre National de la Recherche Scientifique–University of Nantes Unité Mixte de Recherche 6230, F-44322 Nantes, France; [b]Institut de Biologie des Plantes, Centre National de la Recherche Scientifique Unité Mixte de Recherche 8618, Université Paris-Sud, F-91405 Orsay, France; and [c]Institut Universitaire de France, 75005 Paris, France

Edited by Mark H. Thiemens, University of California at San Diego, La Jolla, CA, and approved September 21, 2012 (received for review June 29, 2012)

The stable carbon isotope ^{13}C is used as a universal tracer in plant eco-physiology and studies of carbon exchange between vegetation and atmosphere. Photosynthesis fractionates against $^{13}CO_2$ so that source sugars (photosynthates) are on average ^{13}C depleted by 20‰ compared with atmospheric CO_2. The carbon isotope distribution within sugars has been shown to be heterogeneous, with relatively ^{13}C-enriched and ^{13}C-depleted C-atom positions. The ^{13}C pattern within sugars is the cornerstone of ^{13}C distribution in plants, because all metabolites inherit the ^{13}C abundance in their specific precursor C-atom positions. However, the intramolecular isotope pattern in source leaf glucose and the isotope fractionation associated with key enzymes involved in sugar interconversions are currently unknown. To gain insight into these, we have analyzed the intramolecular isotope composition in source leaf transient starch, grain storage starch, and root storage sucrose and measured the site-specific isotope fractionation associated with the invertase (EC 3.2.1.26) and glucose isomerase (EC 5.3.1.5) reactions. When these data are integrated into a simple steady-state model of plant isotopic fluxes, the enzyme-dependent fractionations satisfactorily predict the observed intramolecular patterns. These results demonstrate that glucose and sucrose metabolism is the primary determinant of the ^{13}C abundance in source and sink tissue and is, therefore, of fundamental importance to the interpretation of plant isotopic signals.

plant $^{13}C/^{12}C$ fractionation | intramolecular isotope distribution | carbohydrate metabolism | enzymatic isotope effects | steady-state modeling

Plants naturally discriminate between ^{12}C and ^{13}C isotopes during CO_2 fixation by photosynthesis: Thus, C_3 plant organic material is on average ^{13}C depleted compared with atmospheric CO_2 (1). (Plant photosynthetic alternative pathways are designated C_3 and C_4. Carbon atom positions in sugars are designated as C-1, C-2, etc.) The amplitude of the isotope fractionation depends on environmental and physiological conditions, notably water deficit, temperature, CO_2 mole fraction, and stomatal conductance (2). Therefore, the natural ^{13}C abundance ($\delta^{13}C$) in plant organic matter has often been used as a physiological marker to investigate plant traits in the field, such as water-use efficiency, photosynthetic capacity, and carbon allocation. {$\delta^{13}C$ (‰) = $1{,}000*[(R_A - R_{V\text{-}PDB})/R_{V\text{-}PDB}]$ is the carbon isotope composition expressed as the deviation of the carbon isotopic ratio ($R = {}^{13}C/{}^{12}C$) of the analyte (R_A) relative to the international standard (Vienna Pee Dee Belemnite, V-PDB ($R = 0.0112372$).} However, the differential incorporation of ^{13}C into various plant compounds and organs is primarily determined by metabolism, which may be accompanied by isotope fractionation. Typically, most heterotrophic tissues have been demonstrated to be ^{13}C enriched by ca. 1‰ compared with photosynthetic tissues. In addition, plant metabolites have contrasting $\delta^{13}C$ values: Cellulose and leaf starch have been shown to be ^{13}C enriched by up to 3‰ (compared with sucrose), whereas lipids are commonly ^{13}C depleted by up to 6‰. Exploiting raw plant organic matter in physiological studies thus appears challenging, because isotopic variations unrelated to the trait being investigated may be caused by tissue composition.

Isotopic disparity among metabolites is caused by metabolic reactions, which discriminate between ^{13}C and ^{12}C isotopes and differentially redistribute C atoms with dissimilar ^{13}C-abundance values (see refs. 3 and 4 for details). A heterogeneous intramolecular $\delta^{13}C$ pattern in source glucose will mean that metabolites derived from glucose metabolism inherit the specific ^{13}C abundance of their precursor C atoms. Such a heterogeneity has been shown by partial (bio)chemical degradation of glucose obtained from beet sugar syrup and isotopic analysis by isotope ratio mass spectrometry (IRMS) of the products (5). Thus, a clear ^{13}C enrichment in the C-atom positions C-3 and C-4 and a clear depletion in C-6 were detected. This pattern partially explains the ^{13}C depletion in fatty acids (derived from C-1 + C-2 and C-5 + C-6) and the enrichment in CO_2 evolved by leaves in the dark (mainly from C-3 and C-4). The ^{13}C enrichment of the C-3 and C-4 positions in glucose has been suggested to originate from the fractionation (that favors ^{13}C) by aldolase (EC 4.1.2.13) during the condensation of two triose phosphate units into fructose-1,6-bisphosphate during photosynthetic glucose synthesis (6).

Nevertheless, despite the fundamental importance of sugars as the main carbon source of plant metabolism, thus as the determinant of the isotopic composition of nearly all metabolites, little progress in understanding the biochemical parameters that define their site-specific $\delta^{13}C$ values has been achieved. It is now 20 y since the pioneering work by Rossmann et al. (5) that unequivocally demonstrated a heterogeneous distribution of ^{13}C in natural glucose. This is primarily because of the technical difficulties inherent in obtaining such information using (bio)chemical degradation coupled with IRMS measurements. Recently, however, ^{13}C NMR spectrometry has been developed that can measure the site-specific ^{13}C abundance in natural glucose, fructose, and sucrose to 1‰ or better (7). The data thus obtained on glucose from beet sucrose were consistent with those of Rossmann et al. (5) quoted above, with the notable exception of the C-1 value. Furthermore, it was shown that fructose and glucose have antisymmetrical $\delta^{13}C$ patterns in C-1 and C-2, thereby suggesting the involvement of isotopic fractionation during their isomerization equilibrium (8). However, the intramolecular pattern of source glucose (starch) or sucrose from leaves rather than a sink tissue has never been measured. Furthermore, the isotope fractionations associated with key enzymes involved in sugar allocation and partitioning within the plant are virtually unknown. Compound-specific analysis with IRMS has suggested that invertase (EC

Author contributions: R.J.R., G.S.R., and G.G.B.T. designed research; A.G. performed research; A.G. and G.S.R. contributed new reagents/analytic tools; A.G., R.J.R., G.S.R., and G.G.B.T. analyzed data; A.G., R.J.R., G.S.R., and G.G.B.T. wrote the paper; and G.G.B.T. carried out modeling.

The authors declare no conflict of interest.

This article is a PNAS Direct Submission.

[1]Present address: Department of Environmental Chemistry and Engineering, Tokyo Institute of Technology, Yokohama 226-8502, Japan.

[2]To whom correspondence should be addressed. E-mail: gilbert.a.aa@m.titech.ac.jp.

This article contains supporting information online at www.pnas.org/lookup/suppl/doi:10.1073/pnas.1211149109/-/DCSupplemental.

3.2.1.26), which cleaves sucrose into glucose and fructose, fractionates against ^{13}C, so that evolved fructose is ^{13}C depleted compared with source sucrose (9). However, the site-specific isotope fractionation of this enzyme has yet to be elucidated. Clearly therefore, the relative roles of glucose biosynthetic reactions and sucrose metabolism as determinants of the intramolecular ^{13}C pattern in sugars are unknown. Critically, there is presently no evidence that source leaf glucose has a heterogeneous intramolecular ^{13}C pattern as found in glucose from sink tissues.

We have therefore addressed two key questions. First, what are the intramolecular $\delta^{13}C$ distributions in source sugars? Second, what are the isotopic fractionations associated with the pertinent enzymes for sugar interconversions? To respond to these questions, we have carried out measurements with ^{13}C NMR and determined the intramolecular patterns of ^{13}C abundance in glucose from leaf, grain, and root. Because the ^{13}C NMR technique requires substantial amounts of source material, we used the large leaves of cocklebur (*Xanthium strumarium*) to obtain pure leaf starch, wheat (*Triticum aestivum*) grain for storage starch, and sugar beet root (*Beta vulgaris*) to obtain storage sucrose. Further, we have measured the in vitro isotope fractionations associated with the reactions of commercially available invertase (EC 3.2.1.26) and glucose isomerase (EC 5.3.1.5). We have then integrated these experimentally determined fractionations into a model and show that the activities of the key enzymes aldolase, invertase, and glucose isomerase satisfactorily explain the intramolecular patterns observed in both source and sink organs.

Results

Intramolecular ^{13}C Pattern in Starch and Sucrose. A recent method based on an adapted, nonfractionating derivatization procedure blocking configurational changes, combined with quantitative ^{13}C NMR spectrometric analysis (7), gives access to the natural ^{13}C pattern in sugars. This technique has allowed us to determine the intramolecular, site-specific $\delta^{13}C$ in sugars with a precision of 0.9‰ on the δ-scale (7, 8). Due to variations in absolute $\delta^{13}C$ values caused by different sources of photosynthetic carbon, all of the values given here are expressed with respect to the molecular average as $\Delta\delta^{13}C$ values. ($\Delta\delta^{13}C$ is defined as the $\delta^{13}C$ difference between the C-atom position of interest and the molecular average.) The intramolecular ^{13}C pattern in glucose residues from leaf transitory starch is shown in Fig. 1*A*. The observed pattern is similar to that found in sugar beet glucose previously (5, 7), with the exception of a clear difference in C-1, which is ^{13}C enriched by ca. 4‰ compared with the molecular average. The C-6 position is substantially ^{13}C depleted, by about 8‰.

The intramolecular ^{13}C pattern in glucose from wheat grain storage starch is shown in Fig. 1*B*. The pattern is seen to be very different from that in leaf transitory starch, with the C-1 and C-2 positions, respectively, ^{13}C depleted and ^{13}C enriched. In glucose from beet root sucrose (Fig. 1*C*) the ^{13}C pattern is rather similar to that in leaf starch, differing principally in having a more pronounced ^{13}C enrichment in C-4. The ^{13}C pattern in the fructose moiety of the same sucrose is very different from that of the glucose moiety (Fig. 1*D*). C-1 and C-2 are relatively ^{13}C depleted and ^{13}C enriched, implying that the isomerization between glucose and fructose, which involves the C-1 and C-2 positions, causes isotopic alterations.

Isotope Fractionation Introduced by Isomerase and Invertase. The site-specific ^{13}C-isotope fractionations associated with these enzyme activities were measured in vitro. The results are expressed relative to the $\delta^{13}C$ in the C-4 position (Fig. 2). No isotopic change is anticipated at this position, because it is distal to the chemical bonds involved in the reaction.

Glucose isomerization was found to be accompanied by significant site-specific kinetic and thermodynamic isotope effects.

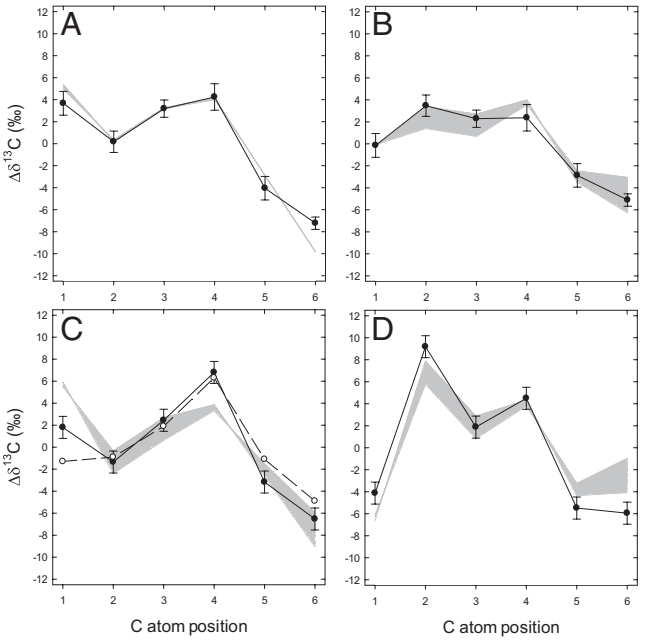

Fig. 1. Intramolecular ^{13}C patterns in glucose measured by site-specific ^{13}C NMR. (*A–D*) Leaf starch (*A*), wheat grain starch (*B*), glucosyl moiety of sugar beet sucrose (*C*), and fructosyl moiety of sugar beet sucrose (*D*). Mean ± SE, $n = 6$. Experimental values (●, ○) are expressed as deviations from the molecular average, $\Delta\delta^{13}C$ (see main text). Shaded areas indicate modeled intramolecular patterns with different parameter values used for calculations: starch synthesis within 10–50% of net carbon fixation in leaves (*A*) or contribution of leaf starch to the buildup of reserves within 50–90% ($L = 0.1$–0.5) (*B–D*). In *C*, values from Rossmann et al. (5) are indicated (○).

For the former, fractionations were measured over a short 1- to 2-h period on the product in the fructose-to-glucose direction and for the latter when reaction had reached equilibrium (*Materials and Methods*). When measured in the fructose-to-glucose direction, the reaction was accompanied by a significant normal kinetic isotope effect of ca. 15‰ in C-2 (Fig. 2*A*). (A normal isotope effect selects against the substrate molecules with ^{13}C at that position, leading to a lower $^{13}C/^{12}C$ ratio at that position in the product. An inverse isotope effect selects in favor of substrate molecules with ^{13}C at that position.) This indicates that, during the isomerization of glucose to fructose (forward reaction), evolved fructose molecules will be ^{13}C depleted by 15‰ in C-2 compared with the corresponding position in glucose. The thermodynamic isotope fractionations, which are independent from the enzyme, manifest themselves when the reaction has reached equilibrium. Again relative to fructose as initial substrate, at equilibrium there was a normal thermodynamic isotope effect in C-2 and C-6 (ca. 7‰ and 4‰, respectively) and an inverse thermodynamic isotope effect in C-1 (ca. 13‰) (Fig. 2*A*). Overall, therefore, the isomerization of fructose to glucose (backward reaction) fractionated against ^{13}C by ca. 18‰ in C-1 and ca. 8‰ in C-2. Taken as a whole, glucose isomerization to fructose tends to enrich in ^{13}C the C-1 in glucose and the C-2 in fructose. These results are in agreement with thermodynamic potentials that explain the systematic enrichment in carbonyl compared with hydroxyl groups (10, 11).

The invertase reaction was accompanied by a kinetic isotope fractionation against ^{13}C (ca. 7‰) in the C-2 position of the fructosyl moiety: There was no significant effect in any other site. Because invertase is not reversible, there is no possible thermodynamic isotope fractionation. The fractionation in C-2 obtained here agrees with the chemical mechanism of the reaction, which is predicted to involve a primary ^{13}C isotope effect only in this position (9).

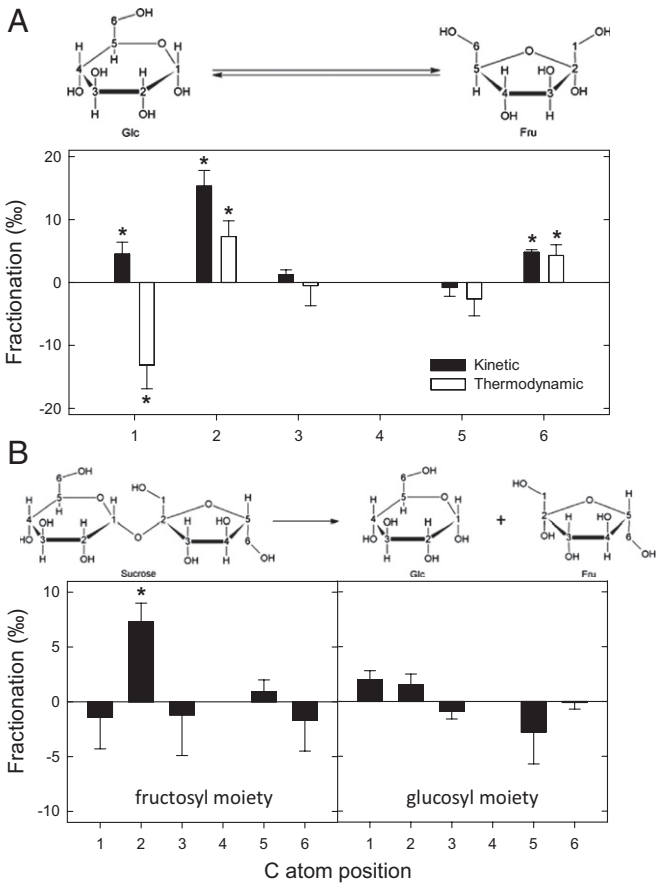

Fig. 2. (*A* and *B*) Site-specific $^{12}C/^{13}C$ isotope fractionation (‰) of the glucose isomerase (*A*) and the invertase (*B*) reactions assayed in vitro. Asterisks indicate fractionations significantly different from zero ($P < 0.05$). For invertase, there is no thermodynamic measurement because the reaction is irreversible. In both cases, fractionation values are relative to that in C-*4*; that is, it was assumed that no fractionation occurred at the C-4 position because no net chemical event takes place at this site. Positive values indicate a fractionation against ^{13}C, and negative values indicate a fractionation in favor of ^{13}C.

We recognize that the enzymes studied here were not from plants but from microorganisms (*Streptomyces*, *Saccharomyces*). In particular, plant glucose isomerase uses glucose-6-phosphate as substrate, not glucose. Nevertheless, the chemical mechanisms of the plant counterparts are the same. Although some differences in the $^{12}C/^{13}C$ isotope effect of enzymes from different biological origins have been reported (12, 13), it seems reasonable to anticipate isotope effects of the same degree for the plant and microbial enzymes.

Isotope ^{13}C-Distribution Patterns Obtained by Modeling. The model previously described for analyzing ^{13}C allocation in plant metabolism in the steady state (14) was extended to integrate the metabolic reactions of sugar interconversions (depicted in Fig. 3) (*SI Text*). The output of the model is the site-specific $\delta^{13}C$ pattern in glucose, fructose, and sucrose. Due to the difference in intramolecular pattern in leaf cytoplasmic day sucrose and in starch-derived night sucrose, the model depends upon the nature of source sucrose (day or night) used to accumulate grain starch or root sucrose. The robustness of the model was then explored, using different levels of prevalence of day or night sucrose (shaded area in Fig. 1 *B–D*).

Discussion

It has previously been demonstrated that the ^{13}C distribution within plant sugars and primary storage carbohydrates is not homogeneous and that this heterogeneity is maintained in metabolites derived from these primary carbon sources (3, 4). It is now apparent that an analysis of the mean $\delta^{13}C$ distribution (molecular average) in source sugars is insufficient to link effectively $\delta^{13}C$ values to plant metabolism. First, it is clear that there is sugar-specific variation in the intramolecular $\delta^{13}C$ distribution in source sugars, which will vary dependent on the source involved. Second, it is evident that this variation will be governed by isotopic fractionations associated with enzymes involved in sugar interconversions. It remains to be unraveled to what extent the intrinsic enzyme properties and metabolic-pathway–related C partitioning will impact the $\delta^{13}C$ distribution determined in metabolites.

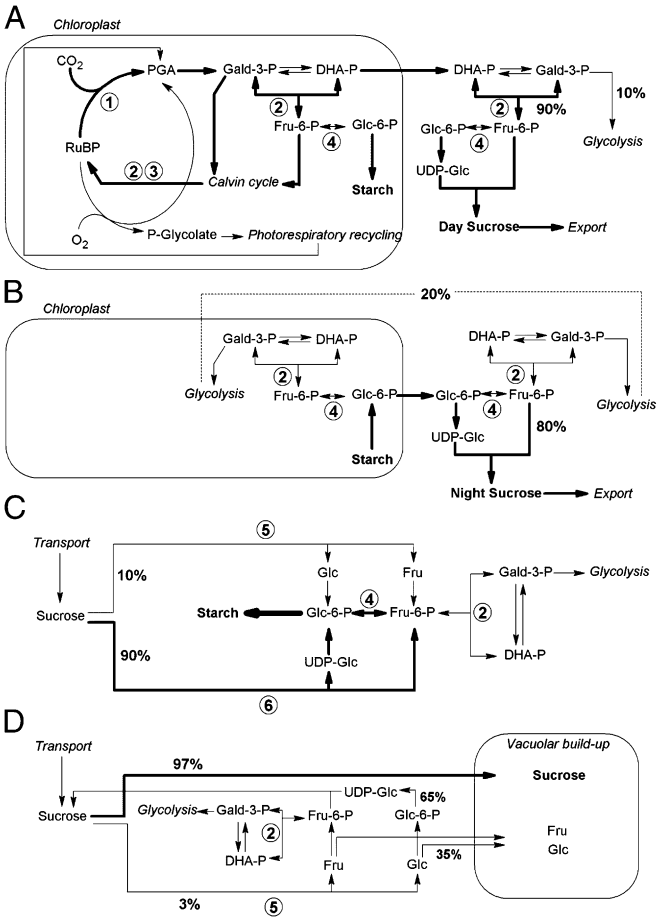

Fig. 3. (*A–D*) Simplified scheme showing the important steps of sugar metabolism in the illuminated leaf (*A*), the darkened leaf (*B*), wheat grain (*C*), and beet root (*D*). 1, ribulose-1,5-bisphosphate carboxylase/oxygenase; 2, (trans)aldolase; 3, transketolase; 4, phosphoglucose isomerase; 5, invertase; 6, sucrose synthase. In *A–D*, the major pathway is indicated with thick arrows. Known partition factors are given (%); for example, in *B*, the commitment of fructose to glycolysis represents about 20% of total fructose utilization; in *D*, 35% of glucose produced by invertase accumulates in the vacuole whereas 65% reforms sucrose. In *C* and *D*, source sucrose comes from *A* and *B*, with variable proportions (main text and Fig. 1 legend). Abbreviations: DHA-P, dihydroxyacetone phosphate; Gald-3-P, 3-phosphoglyceraldehyde; PGA, 3-phosphoglyceric acid. For clarity, bis-phosphorylated intermediates are not shown.

Involvement of Enzymes in Defining Intramolecular ^{13}C Patterns in Primary Sugars. In general, there is a relative enrichment of the C-3 and C-4 positions compared with the average of the other positions. This enrichment is particularly clear in the glucose residue of cocklebur starch (Fig. 1*A*) and the glucosyl moiety of sugar beet sucrose (Fig. 1*C*). During photosynthetic carbon metabolism, these positions are derived from triose phosphates through condensation by aldolase to form fructose-1,6-bisphosphate (Fig. 3, reaction 2), a reaction that is known to favor ^{13}C (6). Indeed, the equilibrium isotope fractionation for the rabbit muscle aldolase has been shown to be, respectively, 3.6‰ and 4.9‰ in favor of ^{13}C in C-3 and C-4. Back calculation from the isotope distribution in glucose obtained by Rossmann et al. (5) and from β-factors (thermodynamic potential) has arrived at larger values, up to 18‰ (14). Here, the comparison of positional average values (C-3 + C-4 vs. C-1 + C-2 + C-5 + C-6) suggests an effective fractionation in favor of ^{13}C in C-3 + C-4 of ca. 10‰.

However, the aldolase reaction is certainly not the sole actor in the determination of intramolecular ^{13}C patterns, because the C-6 is systematically ^{13}C depleted and the C-1 and C-2 positions vary antisymmetrically (Fig. 1 *C* and *D*). Hexose metabolism is certain to be influenced by the isomerization equilibrium between glucose-6-phosphate and fructose-6-phosphate, because such a conversion is required to synthesize sucrose or starch (Fig. 3). We show here that glucose isomerase is accompanied by both a thermodynamic and a kinetic isotope effect (Fig. 2*A*). When equilibrium is reached, the C-1 in glucose and the C-2 in fructose are ^{13}C enriched.

Other enzymes are also likely to influence the ^{13}C pattern in sugars. Notable among these is invertase, which cleaves sucrose into glucose and fructose and fractionates against ^{13}C, thereby depleting the C-2 position in fructose (Fig. 2*D*). However, the impact of fractionation introduced by invertase will vary depending on the tissue. Thus, in beet roots the effect is rather small because the proportion of sucrose molecules hydrolyzed by invertase is only ca. 3%, the rest being cleaved by sucrose synthase (EC 2.4.1.13) (Fig. 3*C*) (15, 16). The chemical mechanism of the latter does not involve the cleavage or creation of a C-C bond and therefore is unlikely to discriminate significantly between carbon isotopes at the level of the fructose moiety (secondary isotope effect) (17). (A primary isotope effect is associated with the atoms involved in the cleavage or formation of a bond. Secondary isotope effects occur due to isotopic substitution in adjacent atoms that are only indirectly involved in the reaction.) In addition, the possible fractionation against ^{13}C in C-1 of the glucose moiety is counterbalanced by the very large commitment of this reaction (97%; Fig. 3*C*, reaction 6). Similarly, the sucrose phosphate synthase (EC 2.4.1.4) that forms sucrose phosphate from UDP-glucose and fructose-6-phosphate cannot fractionate in C-1 of the glucosyl moiety, because UDP-glucose is essentially fully committed to sucrose production.

Triose phosphate isomerization, the interconversion of 3-phosphoglyceraldehyde and dihydroxyacetone phosphate, may also introduce isotope fractionation. However, the kinetic fractionation in carbon is certain to be small, because the limiting step of the reaction [proton transfer to the active site (18)] again does not involve a primary carbon isotope effect. The thermodynamic fractionation is probably also negligible, due to the free energy associated with the reaction, which leads to a ratio of 3-phosphoglyceraldehyde to dihydroxyacetone phosphate of 3:97 (19): that is, to a nearly complete conversion of 3-phosphoglyceraldehyde into dihydroxyacetone phosphate. In photosynthesis, dihydroxyacetone phosphate is synthesized extremely rapidly from 3-phosphoglyceraldehyde by the very efficient enzyme triose phosphate isomerase ($k_{cat}/K_m \sim 10^5$ $L{\cdot}mol^{-1}{\cdot}s^{-1}$), thereby preventing any $^{12}C/^{13}C$ isotope fractionation with respect to source phosphoglycerate. In addition, should the fractionation be large or significant, then the C-2 position in leaf glucose would be considerably enriched: The evidence is quite to the contrary (Fig. 1*A*).

Metabolic Pathways and Partitioning in Carbohydrate Metabolism. The combination of the known metabolic pathways (Fig. 3) and the isotope fractionation values discussed above allows us to predict the ^{13}C patterns in sugars from equations based on steady-state conditions (shaded areas in Fig. 1; see *SI Text* for calculation details). Calculations nevertheless depend on physiological parameters, such as the proportion of day sucrose vs. night sucrose (denoted as L in the model) (*SI Text*) used to accumulate starch or sucrose in wheat and beet, respectively, because the modeled ^{13}C patterns in day and night sucrose are different. Regrettably, specific data on diurnal kinetics of grain starch synthesis or beet sucrose accumulation are scarce. Available data indicate that sucrose accumulation and growth are more intense in beet root during the night (20, 21) and that in wheat grains, starch accumulation is privileged in the night, whereas cell division and cell wall synthesis occur in the light (22, 23). Therefore, the calculations were carried out with a prevalence of night sucrose (larger utilization of sucrose synthesized from leaf starch remobilization: $L < 0.5$). The predicted values are not very sensitive to L, however, as seen from the relatively narrow shaded areas in Fig. 1 *B–D*. Similarly, in leaves the predicted ^{13}C pattern in starch is not very sensitive to variations in the starch synthesis rate (Fig. 1*A*). The agreement between modeled and measured ^{13}C patterns is generally very satisfactory, with no $\Delta\delta^{13}C$ difference of more than 4‰. Particularly noteworthy is that the patterns generated by the model match very closely the ^{13}C depletion in the C-6 position of glucose compared with the C-1, a difference that up to now has been poorly understood (5, 14, 24). In the framework of the model, this clearly demonstrates that the isotopic difference between these two positions principally originates from the ^{13}C enrichment in C-1 caused by the isomerization equilibrium between glucose and fructose (Fig. 2). In the steady state, invertase further tends to ^{13}C deplete free fructose accumulated in the vacuole and to cause a ^{13}C enrichment in fructose recycled to sucrose. Accordingly, the modeled $\Delta\delta^{13}C$ values in C-1 and C-2 of fructose from sugar beet sucrose that result from the combined action of invertase and isomerase (Fig. 3*D*) reflect perfectly the observed values (Fig. 1*D*).

Of course, the present calculations cannot be considered to be fully representative in that they are derived from a model that does not integrate all of the complexities of sugar metabolism and partitioning in plants, such as pentose phosphate metabolism. For example, there is currently considerable uncertainty as to the specific source of carbon used to synthesize starch in cereals and the possible involvement of stem and culm reserves (mainly in the form of fructans) (25, 26). Should fructans be involved in wheat grain filling, their impact on the isotopic pattern in starch would be a ^{13}C enrichment (nonfractionating remobilization of "old" fructans), a ^{13}C depletion (conversion of fructose into fructans), or no effect at all (steady fructan pool) in the C-2 position. Further data on the $\delta^{13}C$ in fructans and the dynamics of fructan pools would thus be necessary to improve our current model of the intramolecular ^{13}C pattern in wheat sugars. In addition, in both beet and wheat, carbon partitioning to sucrose and starch, respectively, seems to be highly sensitive to environmental conditions, such as day and night temperature (20, 27) and water stress (28, 29). Plant responses to environmental conditions encompass changes in enzyme activity including invertase (e.g., in maize, ref. 30). We recognize that our analysis is based on typical documented partition factors and commitments largely obtained from plants grown under experimental conditions. In the field, intramolecular ^{13}C patterns may vary with different plant culture conditions or crop varieties.

Consequences of Intramolecular ^{13}C Patterns in Primary Sugars on Plant Metabolites. The intramolecular heterogeneous distribution of ^{13}C in glucose and fructose has pervading consequences for ^{13}C isotopic distribution in plants, because all of the downstream

metabolites inherit the isotopic composition of their metabolic source. Well-known examples are the ^{13}C enrichment in leaf-respired CO_2 and the overall ^{13}C depletion in fatty acids (see ref. 24 for a discussion), which derive from C-3 + C-4 and C-1 + C-2 + C-5 + C-6 positions of glucose, respectively. It is interesting to note that the intramolecular variation in ^{13}C isotopic distribution in glucose also plays a role in defining the well-established alternating site-specific ^{13}C distribution in fatty acids, described both for bacteria (31) and for plants (32) and previously assigned principally to kinetic isotope effects in the pyruvate dehydrogenase reaction (31, 33).

In this study, we show that source glucose used in darkened leaves (remobilized from starch) is ^{13}C enriched in the C-1 position. The decarboxylation of this carbon atom by the pentose phosphate pathway should produce ^{13}C-enriched carbon dioxide, unless an effective isotope fractionation against ^{13}C by the associated decarboxylase [phosphogluconate dehydrogenase (decarboxylating) EC 1.1.1.44] occurs (34, 35). In contrast, the ^{13}C depletion in C-6 should impact on C atoms in metabolites: For example, carboxylic groups in histidine and tryptophan or the formyl (or methylene) group exchanged in C_1 metabolism, which come from the C-1 and C-6 positions. We further postulate that such isotopic consequences are dissimilar between plant organs because the $\Delta\delta^{13}C$ values are different. For instance, CO_2 evolved by pyruvate dehydrogenase (EC 1.2.4.1), the first decarboxylation step of respiration, should be relatively more ^{13}C enriched in sugar beet root than in wheat grains (Fig. 1). Similarly, metabolites formed from glycolytic acetyl-CoA should be more ^{13}C depleted in beet root than in wheat grains. In other words, in addition to tissue composition being variable between organs, the intramolecular pattern may cause changes in the natural ^{13}C abundance of organic matter (3, 36–38). Our results show that the metabolism of sucrose taking place in sink organs has clear effects on the ^{13}C pattern: The less heterogeneous pattern in wheat grain should lead to smaller isotopic differences among downstream metabolites than in sugar beet roots.

Other metabolic pathways can have a significant influence on the ^{13}C signal of plant tissues. Glucose derived from C_4 plant metabolism does not seem to have the same ^{13}C distribution as that from C_3 plants (5, 7). In addition, anaplerotic carbon fixation by phospho*enol*pyruvate carboxylase (PEPc; EC 4.1.1.31) leads to a positional ^{13}C enrichment in organic acids and amino acids (3). The PEPc activity has been shown to vary between plant parts and this might correlate with the well-documented ^{13}C enrichment in sink organs (39, 40). Because organic acids are key intermediates involved in respiration and in the biosynthesis of amino acids, their intramolecular ^{13}C pattern is thus of importance to better understand the ^{13}C distribution within plants. This needs to be addressed in the future.

Materials and Methods

Chemicals. Silica (63- to 200-μm mesh), TLC plates (aluminum sheets, silica gel 60 F_{254}), acetic acid (99% vol/vol), ethanol (99% vol/vol), magnesium sulfate pentahydrate, charcoal, and celite were purchased from VWR. Glucose isomerase (EC 5.3.1.5) immobilized from *Streptomyces murinus*, invertase (EC 3.2.1.26) from baker's yeast (*Saccharomyces cerevisiae*), amyloglucosidase (EC 3.2.1.3) from *Aspergillus niger*, and acetonitrile (HPLC quality) were purchased from Sigma Aldrich. Sodium acetate was from Fluka.

Plant Growth Conditions. *Xanthium strumarium* L. were grown from seeds in the greenhouse as described in ref. 41. After 2 mo, mature leaves (ranks 5 and 6 from the apex) were collected in the light and immediately frozen in liquid nitrogen for starch extraction.

Starch Extraction and Hydrolysis. Starch was purified from leaves as described in ref. 42 with acid gelatinization (HCl) and precipitation in cold methanol. Samples were then lyophilized for further analysis. One gram of pure starch (representing 30 leaves) was placed in 10 mL of acetate buffer (pH 4.6). The mixture was then autoclaved (120 °C; 1 bar) for 30 min to gelatinize the starch. Ten milliliters of acetate buffer and 20 mg of amyloglucosidase from *Aspergillus niger* were added. The medium was heated at 60 °C and the reaction was followed by TLC on silica plates (AcOEt/MeOH/H_2O 7:2:1). After starch disappearance (ca. 2 h), the solution was filtered on a celite/silica bed (1 cm). The filtrate was then evaporated and coevaporated with ethanol to obtain a syrup that was used without further purification for glucose derivatization.

Sugar Quantitation by HPLC. Sugars were analyzed by high pressure liquid chromatography on an NH_2 column (Phenomenex) equipped with a loop injector (20 μL) and a refractometer. Elution was made with a mixture of CH_3CN/H_2O (80:20) at a flow rate of 1mL/min at room temperature.

Isomerase Assay. The reaction medium was prepared with 500 mL of distilled water containing 1.5 g of $MgSO_4{\cdot}5H_2O$ at pH 7.5 (adjusted with $NaHCO_3$). To 100 mL of the medium was added 17 g of either glucose or fructose and the medium was stirred at 60 °C for 30 min. Immobilized glucose isomerase (400 mg, 350 units/mg) was then added and the reaction was followed by HPLC (see above). The chemical equilibrium was reached in ca. 24 h and the ratio of fructose to glucose was 1:1. To stop the reaction, the medium was filtered on a 0.22-μm filter. The resulting filtrate was evaporated to yield a syrup, which was used without further purification for glucose and fructose derivatization. For the determination of equilibrium isotope effects, the reaction was followed for 3 or 10 d and both fructose and glucose were used as substrates. For the determination of kinetic isotope effects, the reaction was run with fructose as the substrate and was stopped at different times (1–2 h).

Invertase Assay. One milliliter of a 5-mg/mL (300 units/mg) invertase solution in water was added to 100 mL of sucrose solution (0.43 M) at room temperature. The reaction was quenched at different times (between 50 and 120 min) by adding 0.5 mL of 1 mM NaOH. Sucrose, glucose, and fructose concentrations were followed by HPLC.

Sucrose Isolation. To the quenched invertase assay was added 15 g of activated charcoal. The mixture was stirred for 15 min at room temperature and then placed at 4 °C for 1 h. The mixture obtained was deposited on a charcoal celite column (40 g charcoal; 40 g celite, conditioned with distilled water) equipped with a vacuum flask (flow rate of ca. 10 mL/min). Elution was carried out with pure water, ethanol/water (1:99), ethanol/water (5:95), and then pure ethanol until all of the sucrose had eluted. The fractions were then evaporated and dried over P_2O_5 in a desiccator overnight before derivatization.

Carbohydrate Derivatization and NMR Analysis. The carbohydrates (glucose, fructose, and sucrose) were converted to glucose and fructose acetonide derivatives and were analyzed by quantitative ^{13}C NMR spectrometry as described previously (7, 8).

Calculation of Isotope Effects. Kinetic isotope effects were calculated from experimental data, using equations describing isotopic Rayleigh effects (43). The positional isotope effect values were calculated assuming a negligible isotope effect on the C-4 position of both glucose and fructose (Fig. 2).

Modeling. The calculation of the site-specific carbon isotope composition (^{13}C pattern) was carried out using the model of Tcherkez et al. (14), completed with the isotope fractionations of glucose isomerization found here (Fig. 3 *A* and *B*). Day and night sucrose (output of the model) were used as source sucrose to compute the ^{13}C pattern in starch and sucrose in wheat grain and sugar beet root, respectively, with the metabolic pathways considered in Fig. 3 *C* and *D* and the isotope fractionation by aldolase, invertase, and isomerase. In all cases, the fractionation by starch synthase, glycolysis, and sucrose synthase (SuSy) was assumed to be negligible and the metabolism was assumed to be in the steady state (see *SI Text* for further details).

ACKNOWLEDGMENTS. The authors acknowledge the financial support of the Centre National de la Recherche Scientifique, of the Région Pays de la Loire, and of the French Agence Nationale de la Recherche through project Jeunes Chercheurs, under Contract JC08-330055.

1. Brugnoli E, Farquhar GD (2000) *Photosynthesis: Physiology and Metabolism*, eds Leegood C, Sharkey TD, von Caemmerer S (Kluwer Academic, The Netherlands), pp 399–434.

2. Farquhar GD, Ehleringer JR, Hubick KT (1989) Carbon isotope discrimination and photosynthesis. *Annu Rev Plant Physiol Plant Mol Biol* 40:503–537.

3. Schmidt H-L, et al. (1995) *Stable Isotopes in the Biosphere*, eds Wada E, Yoneyama T, Minagawa M, Ando T, Fry B (Kyoto Univ Press, Kyoto, Japan), pp 17–35.
4. Schmidt H-L, Gleixner G (1998) *Stable Isotopes. Integration of Biological, Ecological and Geochemical Processes*, ed Griffiths H (BIOS Scientific, Oxford), pp 13–25.
5. Rossmann A, Butzenlechner M, Schmidt HL (1991) Evidence for a nonstatistical carbon isotope distribution in natural glucose. *Plant Physiol* 96(2):609–614.
6. Gleixner G, Schmidt H-L (1997) Carbon isotope effects on the fructose-1,6-bisphosphate aldolase reaction, origin for non-statistical 13C distributions in carbohydrates. *J Biol Chem* 272(9):5382–5387.
7. Gilbert A, Silvestre V, Robins RJ, Remaud GS (2009) Accurate quantitative isotopic ^{13}C NMR spectroscopy for the determination of the intramolecular distribution of ^{13}C in glucose at natural abundance. *Anal Chem* 81(21):8978–8985.
8. Gilbert A, Silvestre V, Robins RJ, Tcherkez G, Remaud GS (2011) A ^{13}C NMR spectrometric method for the determination of intramolecular $\delta^{13}C$ values in fructose from plant sucrose samples. *New Phytol* 191(2):579–588.
9. Mauve C, et al. (2009) Kinetic $^{12}C/^{13}C$ isotope fractionation by invertase: Evidence for a small *in vitro* isotope effect and comparison of two techniques for the isotopic analysis of carbohydrates. *Rapid Commun Mass Spectrom* 23(16):2499–2506.
10. Urey HC (1947) The thermodynamic properties of isotopic substances. *J Chem Soc* 562–581.
11. Cleland WW (2005) The use of isotope effects to determine enzyme mechanisms. *Arch Biochem Biophys* 433(1):2–12.
12. Tcherkez G, Farquhar GD, Andrews TJ (2006) Despite slow catalysis and confused substrate specificity, all ribulose bisphosphate carboxylases may be nearly perfectly optimized. *Proc Natl Acad Sci USA* 103:7246–7251.
13. Schramm VL (2007) Enzymatic transition state theory and transition state analogue design. *J Biol Chem* 282(39):28297–28300.
14. Tcherkez G, Farquhar G, Badeck F, Ghashghaie J (2004) Theoretical considerations about carbon isotope distribution in glucose of C_3 plants. *Funct Plant Biol* 31:857–877.
15. Giaquinta R (1977) Sucrose hydrolysis in relation to phloem translocation in *Beta vulgaris*. *Plant Physiol* 60(3):339–343.
16. Lemoine R, Daie J, Wyse R (1988) Evidence for the presence of a sucrose carrier in immature sugar beet tap roots. *Plant Physiol* 86(2):575–580.
17. Zheng Y, Anderson S, Zhang Y, Garavito RM (2011) The structure of sucrose synthase-1 from *Arabidopsis thaliana* and its functional implications. *J Biol Chem* 286(41):36108–36118.
18. Leadlay PF, Albery WJ, Knowles JR (1976) Energetics of triosephosphate isomerase: Deuterium isotope effects in the enzyme-catalyzed reaction. *Biochemistry* 15(25): 5617–5620.
19. Bassham JA, Krause GH (1969) Free energy changes and metabolic regulation in steady-state photosynthetic carbon reduction. *Biochim Biophys Acta* 189(2):207–221.
20. Ohki K, Ulrich A (1973) Sugarbeet growth and development under controlled climatic conditions with reference to night temperature. *J Sugar Beet Res* 17:270–279.
21. Ulrich A (1952) The influence of temperature and light factors on the growth and development of sugar beets in controlled climatic environments. *Agron J* 44:66–73.
22. Cruz-Aguado JA, Rodés R, Ortega E, Pérez IP, Dorado M (2001) Partitioning and conversion of ^{14}C-photoassimilates in developing grains of wheat plants grown under field conditions in Cuba. *Field Crops Res* 69:191.
23. Jiang D, Cao W-X, Dai T-B, Jing Q (2004) Diurnal changes in activities of related enzymes to starch synthesis in grains of winter wheat. *Acta Bot Sin* 46:51–57.
24. Gilbert A, Silvestre V, Robins RJ, Remaud GS, Tcherkez G (2012) Biochemical and physiological determinants of intramolecular isotope patterns in sucrose from C_3, C_4 and CAM plants accessed by isotopic ^{13}C NMR spectrometry: A viewpoint. *Nat Prod Rep* 29(4):476–486.
25. Scofield GN, et al. (2009) Starch storage in the stems of wheat plants: Localization and temporal changes. *Ann Bot (Lond)* 108:17550–17555.
26. Schnyder H (1993) The role of carbohydrate storage and redistribution in the source-sink relations of wheat and barley during grain filling—A review. *New Phytol* 123: 233–245.
27. Zhao H, Dai T, Jiang D, Cao W (2008) Effects of high temperature on key enzymes involved in starch and protein formation in grains of two wheat cultivars. *J Agron Crop Sci* 194:47–54.
28. Ahmadi A, Baker DA (2001) The effect of water stress on the activities of key regulatory enzymes of the sucrose to starch pathway in wheat. *Plant Growth Regul* 35: 81–91.
29. Monti A, Brugnoli E, Scartazza A, Amaducci MT (2006) The effect of transient and continuous drought on yield, photosynthesis and carbon isotope discrimination in sugar beet (*Beta vulgaris* L.). *J Exp Bot* 57(6):1253–1262.
30. Trouverie J, Thévenot C, Rocher J-P, Sotta B, Prioul J-L (2003) The role of abscisic acid in the response of a specific vacuolar invertase to water stress in the adult maize leaf. *J Exp Bot* 54(390):2177–2186.
31. Monson K, Hayes J (1982) Carbon isotopic fractionation in the biosynthesis of bacterial fatty acids. Ozonolysis of unsaturated fatty acids as a means of determining the intramolecular distribution of carbon isotopes. *Geochim Cosmochim Acta* 46:139–149.
32. Zhou Y, et al. (2010) Biosynthetic origin of the saw-toothed profile in $\delta^{13}C$ and $\delta^{2}H$ of *n*-alkanes and systematic isotopic differences between *n-*, *iso-* and *anteiso*-alkanes in leaf waxes of land plants. *Phytochemistry* 71(4):388–403.
33. Melzer E, Schmidt H-L (1987) Carbon isotope effects on the pyruvate dehydrogenase reaction and their importance for relative carbon-13 depletion in lipids. *J Biol Chem* 262(17):8159–8164.
34. Hermes JD, Roeske CA, O'Leary MH, Cleland WW (1982) Use of multiple isotope effects to determine enzyme mechanisms and intrinsic isotope effects. Malic enzyme and glucose-6-phosphate dehydrogenase. *Biochemistry* 21(20):5106–5114.
35. Cleland WW (2006) *Isotope Effects in Chemistry and Biology*, eds Kohen A, Limbach H-H (CRC Taylor and Francis, Boca Raton, FL), pp 915–930.
36. Tcherkez G, Mahé A, Hodges M (2011) (12)C/(13)C fractionations in plant primary metabolism. *Trends Plant Sci* 16(9):499–506.
37. Hobbie EA, Werner RA (2004) Intramolecular, compound-specific, and bulk carbon isotope patterns in C3 and C4 plants: A review and synthesis. *New Phytol* 161: 371–385.
38. Hayes JM (2001) Fractionation of carbon and hydrogen isotopes in biosynthetic processes. *Rev Mineral Geochem* 43:225–277.
39. Cernusak LA, et al. (2009) Why are non-photosynthetic tissues generally ^{13}C enriched compared with leaves in C_3 plants? Review and synthesis of current hypotheses. *Funct Plant Biol* 36:199–213.
40. Gessler A, et al. (2009) On the metabolic origin of the carbon isotope composition of CO_2 evolved from darkened light-acclimated leaves in *Ricinus communis*. *New Phytol* 181(2):374–386.
41. Tcherkez G, et al. (2008) Respiratory metabolism of illuminated leaves depends on CO_2 and O_2 conditions. *Proc Natl Acad Sci USA* 105(2):797–802.
42. Tcherkez G, et al. (2003) Metabolic origin of carbon isotope composition of leaf dark-respired CO_2 in French bean. *Plant Physiol* 131(1):237–244.
43. O'Leary MH (1981) Carbon isotope fractionation in plants. *Phytochemistry* 20: 553–567.